

PRESENTACION MURAL

Weak lensing analysis of the galaxy cluster RX J1117.4+0743 ([VMF 98] 097)

Elizabeth Johana Gonzalez ^{1,2}, Mariano Dominguez ^{1,2,3},
Diego García Lambas ^{1,2,3}, Osvaldo Moreschi ^{2,4}, Gael Foëx ⁵,
José Luis Nilo Castellón ⁶, María Victoria Alonso ^{1,2,3}

(1) *Instituto de Astronomía, Teórica y Experimental (CONICET-UNC),
Córdoba, Argentina*

(2) *Facultad de Matemática, Astronomía y Física (UNC), Córdoba,
Argentina*

(3) *Observatorio Astronómico, (UNC), Córdoba, Argentina*

(4) *Instituto de Física Enrique Gaviola, (CONICET-UNC), Córdoba,
Argentina*

(5) *Departamento de Física y Astronomía, Universidad de Valparaíso,
Valparaíso, Chile*

(6) *Departamento de Física, Universidad de La Serena, La Serena, Chile*

Abstract. We present a weak lensing analysis of the galaxy cluster RX J1117.4+0743 ([VMF 98] 097) at $z=0.485$, based on data collected with Gemini South Telescope. The cluster was formerly analyzed by Carrasco et al. (2007, ApJ, 664, 777), and they found a large discrepancy between the mass estimated from Xray observations and lensing estimates, exceeding the X-ray mass by more than a factor three. Our result for the mass from the weak lensing analysis is lower than the mass obtained by Carrasco et al. and closer to the X-ray mass.

Resumen. Presentamos el análisis de lente débil del cúmulo de galaxias RX J1117.4+0743 ([VMF 98] 097) situado en $z=0.485$, utilizando observaciones obtenidas por el Telescopio Gemini Sur. El cúmulo fue anteriormente analizado por Carrasco et al. (2007, ApJ, 664, 777), quienes encontraron una gran discrepancia entre la masa estimada a partir de observaciones en rayos X y la obtenida a partir del análisis de lente débil, siendo la masa en X más de tres veces mayor. La masa que obtuvimos a partir del análisis de lente débil es menor que la obtenida por Carrasco et al. y más cercana a la masa obtenida en X.

1. Introduction

Weak and strong gravitational lensing are excellent tools to probe the projected mass distribution of clusters, with strong lensing confined to the central regions of clusters, whereas weak lensing can yield mass measurements for larger radii. Here we present a weak lensing analysis of the galaxy cluster RX J1117.4+0743 - hereafter [VMF 98] 097 - at $z = 0.485$. In this work we adopt when necessa-

ry a standard cosmological model: $H_0 = 70 h_{70} \text{ km s}^{-1} \text{ Mpc}^{-1}$, $\Omega_m = 0.3$, and $\Omega_\Lambda = 0.7$.

2. The pipeline

We perform a pipeline based on python language to make the lensing analysis, from the source detection to the shear profile.

We used SExtractor (Bertin & Arnouts, 1996) for the detection and photometry of the sources. For the object classification in stars, galaxies and false detections, we considered the position of the source in the magnitude/central flux diagram, the FWHM respect to the seeing and the stellarity index (CLASS_STAR parameter).

For the shape measurements we used IM2SHAPE (Bridle et al. 2002). For simplicity, both the PSF and the object are modeled with a single elliptical Gaussian profile. The PSF was determined measuring the shapes of the stars as they are intrinsically pointlike objects. After cleaning the catalogue, we linearly interpolate the local PSF at each object position by averaging the shapes of the five closest stars.

The shear profile was computed by averaging the ellipticities components of background galaxies in concentric annuli around the cluster center (usually assumed to be traced by the brightest galaxy). Spherical symmetry implies that the tangential component (E- mode) traces the reduced shear, while the average of the component tilted at $\pi/4$ relative to the tangential component (B- mode) should be zero for the case of perfect symmetry (see Sec. 4 of Bartelmann & Schneider 2001). We finally estimate the cluster mass by fitting the observed shear profile with the singular isothermal sphere (SIS) and the NFW profile using the formalism given by King & Schneider (2001).

2.1. Validation of the shape measurements with simulated data

To check the performance of our pipeline, we tested it on the DES cluster simulation images publically available (Gill et al. 2009), with good results. This simulation consists of a sets of images, with different grades of difficulty, of sheared galaxies according to a SIS profile with a velocity dispersion of 1250 km s^{-1} .

We checked that our Im2shape implementation can recover point-like objects by applying the PSF correction to each star (Figure ??). Shear profiles for images with high and low noise, are shown in Figure ??.

2.2. [VMF 98] 097

We applied our pipeline to the cluster of galaxies [VMF 98] 097. The analysis was based on data collected with the Gemini Multi Object Spectrograph (GMOS; Hook et al. 2004) in imaging mode at the Gemini South Telescope. The cluster was imaged through the r' and g' SLOAN filters (Fukugita et al. 1996) in optimal observing conditions (seeing disk diameter $\sim 0.7''$). Images were reduced using GEMINI/IRAF package, following the standard procedure. The completeness magnitude is $m_c \sim 26$ in the r band.

Galaxies with $23.0 < r' < m_c + 1.0$, $FWHM > 5$, and ellipticities measured with a precision greater than 0.2, were selected as background galaxies. After this selection, we obtained a galaxy density of 30 arcmin^{-2} .

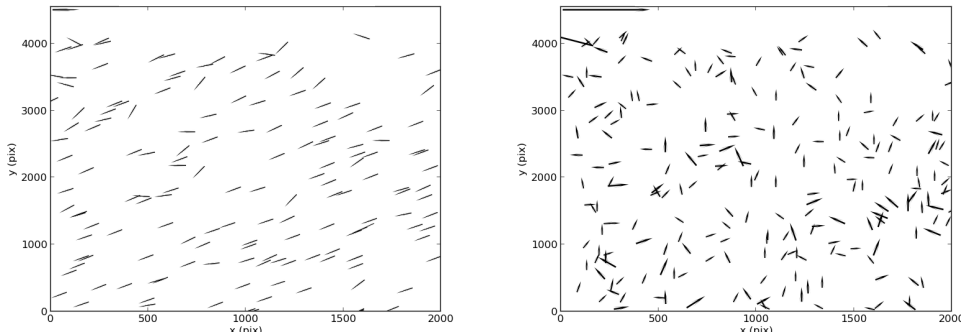


Figure 1. PSF treatment applied to stars of one of the images of the DES simulations: Semiaxis ($a \cos \theta$, $a \sin \theta$) before (*left panel*) and after (*right panel*) the PSF deconvolution, which is more randomly distributed and considerably smaller (the scale is given by the segment in the top-left corner of each panel).

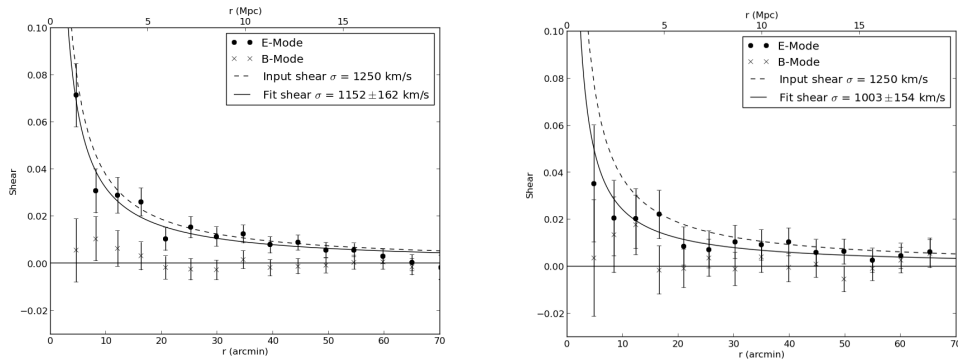


Figure 2. Shear profiles measured on the images with low (*left panel*) and high (*right panel*) noise from the DES cluster simulations. The dashed curve shows the SIS profile for the input value of σ_V and the solid one the fitted profile. The points and crossings show the E and B modes profiles.

To estimate the geometrical factor ($\beta = D_L/D_S$) we used the catalogue of photometric redshifts computed by Coupon et al. 2009. We applied the photometric selection criteria to the catalogue and then we computed $\langle \beta \rangle$ for the whole distribution of field galaxies, taking into account the contamination by foreground galaxies given our selection criteria by setting $\beta(z_{phot} < z_{cluster}) = 0$. We obtained $\langle \beta \rangle = 0.43$. We also used this catalogue to compute the probability that, given the r' magnitude and the color ($g'-r'$), the galaxy was behind the cluster. Using this probability we perform a weighted average of the ellipticity in annular bins to compute the reduced shear.

The centre of the cluster was placed at the brightest galaxy in r' , near the region of higher density of galaxies. For the NFW profile, given that weak lensing analysis alone doesn't give enough constraint in the centre to fit the c parameter, we therefore fixed the concentration parameter $c = 5$, and fit the mass profile

with only one free parameter, R_{200} . At a radius of 0.5 Mpc the inferred weak lensing masses from the r' image are $1.3 \times 10^{14} M_{\odot} h_{70}^{-1}$ and $2.4 \times 10^{14} M_{\odot} h_{70}^{-1}$ for the SIS and NFW profile, respectively (Figure ??).

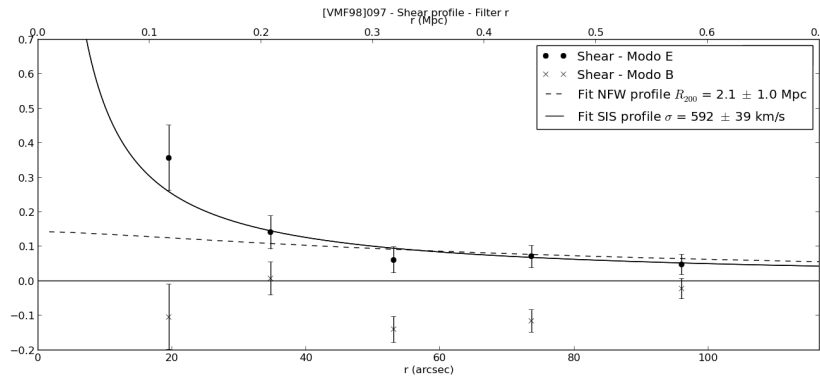


Figure 3. Shear profiles obtained for the r' image of [VMF 98] 097. The solid and the dashed lines represent the best fit of SIS and NFW profiles, respectively. The points and crossings show the E and B modes profiles averaged in annular bins, respectively.

2.3. Conclusion

We have performed a pipeline for the weak-lensing analysis of ground-based images, and tested it on simulated data. Then we applied it to the cluster [VMF 98] 097, which was previously analyzed by Carrasco et al. 2007. We obtained a lower mass that is in better agreement with the X-ray mass ($7.0 \times 10^{13} M_{\odot} h_{70}^{-1}$, Carrasco et al. 2007). Finally, the velocity dispersion of the SIS mass model agrees perfectly the dynamical estimate by Carrasco et al. using spectroscopic images (590 ± 80 km/s).

References

- Bartelmann, M. & Schneider, P. 2001, Phys. Rept., Volume 340, 291, 472
- Bertin, E., Arnouts, S. 1996, A&A Supplement, 117,393
- Bridle, S., Gull, S., Bardeau, S., Kneib, J.P. 2002, in Proc. Yale Cosmology Workshop: The Shapes of Galaxies and their Dark Halos, ed. N. Priyamvada (World Scientific)
- Carrasco E. R., Cypriano E. S., Lima Neto G. B., Cuevas H., Sodre Jr. L., Mendes de Oliveira C. Ramirez A. 2007, ApJ, 664,777
- Coupon, J., Ilbert, O., Kilbinger, M., McCracken, H. J., Mellier Y., et al., 2009, A&A, 500, 981.
- Gill M.S.S., Young J.C., Draskovic J.P., Honscheid K., Lin H., Kuropatkin N., Martini P., Peebles M., Rozo E., Smith G.N., Weinberg D.H. 2009, MNRAS, Submitted [arXiv:0909.3856]
- Hook, I., Jorgensen, I., AllingtonSmith, J. R., Davies, R. L., Metcalfe, N., Murowinski, R. G., Crampton, D. 2004, PASP, 116, 425.
- King, L. J., & Schneider, P. 2001, A&A, 369, 1